arXiv:physics/0207085v2 [physics.atm-clus] 26 Jul 2002

On the applicability of jellium model to the description of alkali clusters

Anton Matveentsev*

A. F. Ioffe Physical-Technical Institute of the Russian Academy of Sciences, Polytechnicheskaya 26, St. Petersburg, Russia 194021

Andrey Lyalin,† Ilia A Solov'yov,‡ Andrey V Solov'yov,§ and Walter Greiner

Institut für Theoretische Physik der Universität Frankfurt am Main, Robert-Mayer 8-10, Frankfurt am Main, Germany 60054

This work is devoted to the elucidation the applicability of jellium model to the description of alkali cluster properties on the basis of comparison the jellium model results with those derived from experiment and within *ab initio* theoretical framework. On the basis of the Hartree-Fock and local-density approximation deformed jellium model we have calculated the binding energies per atom, ionization potentials, deformation parameters and the optimized values of the Wigner-Seitz radii for neutral and singly charged sodium clusters with the number of atoms $N \leq 20$. These characteristics are compared with the results derived from the *ab initio* all-electron simulations of cluster electronic and ionic structure based on the density functional theory as well as on the post Hartree-Fock perturbation theory on many-electron correlation interaction. The comparison performed demonstrates the great role of cluster shape deformations in the formation cluster properties and the quite reasonable level of applicability of the deformed jellium model.

*Email address: anton@rpro.ioffe.rssi.ru

†Permanent address: Institute of Physics, St Petersburg State University, St Petersburg, Petrodvorez, Russia 198504; Email address: lyalin@th.physik.uni-frankfurt.de

‡Permanent address: A. F. Ioffe Physical-Technical Institute, St. Petersburg, Russia 194021; Email address: ilia@th.physik.uni-frankfurt.de

§Permanent address: A. F. Ioffe Physical-Technical Institute, St. Petersburg, Russia 194021; Email address: solovyov@th.physik.uni-frankfurt.de

I. INTRODUCTION

During the last decade, investigation of the detailed structure and properties of small sodium clusters attracted a lot of attention (see, e.g., [1, 2, 3] and references therein), because namely the sodium clusters were used in such important experimental work as the discovery of metal cluster electron shell structure [4] and the observation of plasmon resonances [5, 6, 7]. These experiments were definitely among those, which clearly demonstrated that atomic clusters and small nanoparticles are in fact new physical objects possessing their own properties. The novelty of cluster physics is also greatly connected with the fact that cluster properties explain the transition from single atoms or molecules to solid state. Comprehensive survey of the field can be found in review papers and books, see, e.g., [1, 2, 8, 9, 10, 11, 12].

With the discovery of electronic shell structure in free alkali clusters [4, 13] the essential role of the quantized motion of delocalized valence electrons in the mean field created by ions in a cluster has been understood. Under different experimental conditions, the detailed ionic structure has been found not to affect the properties of alkali and other simple metal clusters very much (see, e.g., [8, 9, 10] for review). This behavior suggests the validity of a jellium model, defined by a Hamiltonian which treats the electrons in the usual quantum mechanical way, but approximates the field of the ionic cores by treating them as a uniform positively charged background. This naturally leads to a description of the electron density in terms of single particle wave functions that extend over the entire cluster.

Initially, jellium calculations for metal clusters were based on the density functional formalism with the use of pseudopotentials for the description of electron relaxation effects and lattice structure [14]. Fully self-consistent calculations for spherical jellium metal clusters have been performed within the framework of the spin-density-functional method [15] and the Kohn-Sham formalism for the self-consistent determination of electron wave functions [13, 16]. The Hartree-Fock (HF) scheme for the self-consistent determination of the electron wave functions of spherical jellium metal clusters was also introduced later in [17, 18].

Shortly after the discovery of electronic shell structure in free alkali clusters [4, 13] it was realized that the detailed size dependence of ionization potentials and other characteristics of small metallic clusters can be understood as a consequence of non-spherical cluster shapes [19] by analogy with the nuclear shell model. Direct evidence for cluster deformation was

achieved in experiments on photoabsorption, where splitting of plasmon resonances caused by cluster deformation was observed (see [8, 9, 10] and references therein).

Kohn-Sham calculations for spherical [13, 16] metal clusters have been generalized for spheroidal [20, 21] and more general axial shapes [22] of light clusters. Light clusters of arbitrary shapes have been studied by means of the "ultimate" jellium model [23, 24]. The Hartree-Fock approach was generalized for axially deformed cluster systems in [25, 26]. The existence of the different shape isomers were discussed in [22, 24, 27]. It was shown that the shape of the magic clusters can deviate from the sphere if higher multipole deformations are taken into account. For example, the magic cluster Na_{40} is not spherical if octupole deformations are allowed. This possibility have been pointed out in [28] and confirmed by the 'ultimate' jellium [29] and the Born-Oppenheimer local-spin density molecular dynamics method [30]. It has been shown that alkali-metal clusters have similar shapes with small atomic nuclei [31]. This similarity is a universal result of the density-functional theory.

The shell-correction method known from nuclear physics [32] has been used in a number of papers in studying spheroidal ground state deformations, energetics, stability towards various fragmentation channels of metal clusters [33, 34, 35, 36]. The role of higher multipole and tri-axial deformations has been elucidated in [37, 38, 39, 40, 41]. Using the shell-correction method, the investigation of metal cluster electronic properties such as binding energies, ionization potentials, electron affinities, energetics of fission channels and systematic comparison of the theoretical results with the available experimental data have been done in [39] (see also [42] and references therein for a review).

Dynamical jellium model for metal clusters, which treats simultaneously collective vibrational modes (volume vibrations, i.e. breathing, and shape vibrations) of the ionic jellium background in a cluster, quantized electron motion and interaction between the electronic and ionic subsystems was developed in [43, 44]. This model allowed the widths of electron excitations in metal clusters beyond the adiabatic approximation to be described.

The jellium model provides a very useful basis for studying various collision processes, such as photabsorption [45], photoionization [46, 47], elastic [48, 49] and inelastic scattering [49, 50, 51, 52], electron attachment [53, 54], photon emission [55, 56], atomic cluster fission process [57, 58] and others, involving metal clusters. On the basis of the jellium model one can develop *ab initio* many-body theories, such as the random phase approximation with exchange or the Dyson equation method and effectively solve many-electron correlation

problem even for relatively large cluster systems containing up to 100 atoms or even more. Review of these methods in their application to the electron scattering of metal clusters one can find in [59]. As elucidated in the papers cited above, many-electron correlations are quite essential for the correct description of various characteristics of the cluster systems.

Structural properties of small metal clusters have been widely investigated using quantum chemistry *ab initio* methods. Here we refer to the papers [3, 60, 61, 62, 63, 64, 65, 66, 67], in which optimized geometries, binding energies, ionization potentials, electron structure and electron transport properties of small lithium and sodium clusters have been calculated.

In spite of the fact that both jellium model results and results of *ab initio* frameworks do exist in literature there have been performed no systematic comparison of the results of the two different theoretical schemes so far. We fill this gap in our present paper and demonstrate that such a comparison is rather illustrative and explains essential physical aspects of the formation of various cluster characteristics and properties. Also, we compare the results of the Hartree-Fock and local-density approximation (LDA) deformed jellium models and on this basis elucidate the role of many-electron correlation effects in the formation of cluster deformations.

On the basis of comparison of the jellium model results with those derived within the *ab initio* theoretical framework and experiment we elucidate the level of applicability of the jellium model to the description of alkali cluster properties. For neutral and singly charged sodium clusters with $N \leq 20$, we have calculated on the basis of Hartree-Fock and LDA deformed jellium model the binding energies per atom, ionization potentials, parameters of deformation and optimized values of the Wigner-Seitz radii. These characteristics are compared with the results derived from the *ab initio* all-electron theoretical framework for the calculation of the cluster ionic and electronic structure based on the density functional theory as well as on the post Hartree-Fock perturbation theory on many-electron correlation interaction. Comparison performed in our work demonstrates the great role of cluster deformations in the formation cluster properties and the quite reasonable level of applicability of the deformed jellium model.

Our paper is organized as follows. In section II, we provide a brief review of theoretical approaches and methods used in the calculation. In section III, we present and discuss jellium and *ab initio* results and make their comparison. In section IV, we draw a conclusion to this paper.

We use the atomic system of units $\hbar = |e| = m_e = 1$ in this paper.

II. THEORETICAL METHODS

In this work we calculate the binding energies per atom, ionization potentials, deformation parameters and the optimized values of the Wigner-Seitz radii for neutral and singly charged sodium clusters with $N \leq 20$ using the Hartree-Fock and LDA deformed jellium model. The jellium model results are compared with those derived in [3] on the basis of *ab initio* all-electron simulations of the cluster electronic and ionic structure. Below we present a brief review of the theoretical methods used in our work. Since the main part of calculations have been done within the framework of the deformed jellium model, we focus in our brief review on the jellium model approach rather than on the details of the more sophisticated *ab initio* methods for which we refer to [3].

A. Two-centered jellium model and cluster shape parameterization

According to the main postulate of the jellium model, the electron motion in a metallic cluster takes place in the field of the uniform positive charge distribution of the ionic background. Originally, the Hartree-Fock model for metal-cluster electron structure has been worked out in the framework of spherically symmetric jellium approximation in [17, 18]. It is valid for clusters with closed electronic shells that correspond to magic numbers (8, 20, 34, 40, 58,...). For metal clusters with arbitrary number of valence electrons an open-shell two-center jellium Hartree-Fock approximation has been developed (see [25, 26, 57]). The two-centered jellium method treats the quantized electron motion in the field of the spheroidal ionic jellium background, whose principle diameters a and b can be expressed as follows:

$$a = \left(\frac{2+\delta}{2-\delta}\right)^{2/3} R, \qquad b = \left(\frac{2-\delta}{2+\delta}\right)^{1/3} R. \tag{1}$$

$R = r_s N^{1/3}$ is the radius of an undeformed spherical cluster with N atoms, r_s is the Wigner-Seitz radius, which for the bulk sodium is equal to 4.0. The deformation parameter δ characterizes the families of the prolate ($\delta > 0$), and the oblate ($\delta < 0$) spheroids of equal volume $V_c = 4\pi ab^2/3 = 4\pi R^3/3$.

The electrostatic potential U of the ionic background can be determined from the solution of the corresponding Poisson's equation:

$$\Delta U(\mathbf{r}) = -4\pi\rho(\mathbf{r}), \tag{2}$$

where

$$\rho = \begin{cases} \rho_c, & (x^2+y^2)/b^2 + z^2/a^2 \leq 1 \\ 0, & (x^2+y^2)/b^2 + z^2/a^2 > 1 \end{cases} \tag{3}$$

describes a uniform distribution of the ions charge density in the volume of the cluster. Here $\rho_c = Z_c/V_c$ is the ionic charge density inside the cluster, and Z_c is the total charge of the ionic core.

B. Hartree-Fock and LDA formalism

The Hartree-Fock equations can be written out explicitly in the form (see, e.g., [68])

$$(-\Delta/2 + U + U_{HF}) \mid a >= \varepsilon_a \mid a > . \tag{4}$$

The first term here represents the kinetic energy of electron a, and U its attraction to the cluster core. The Hartree-Fock potential U_{HF} represents the average Coulomb interaction of electron a with the other electrons in the cluster, including the non-local exchange interaction, and ε_a describes the single electron energy.

According to the density-functional theory, the ground state energy reaches its minimum as a function of the density of the system at the exact density [69]. A self-consistent method for calculation of the electronic states of many-electron systems was proposed by Kohn and Sham [70]. This method leads to the Kohn-Sham LDA self-consistent equations:

$$(-\Delta/2 + U + U_H + V_{xc}) \mid a >= \varepsilon_a \mid a > . \tag{5}$$

Here U_H is the Hartree potential, which represents the direct Coulomb interaction of electron a with other electrons in the cluster, but does not take into account the non-local exchange effects, while V_{xc} is the phenomenological density dependent local exchange-correlation potential. The important feature of the LDA method consist in the fact that it takes into account many-electron correlations (see, e.g., [71, 72] for review). In the present

work we use the Gunnarsson and Lundqvist model [73] for the LDA electron exchange-correlation energy density ϵ_{xc}, which reads as

$$\epsilon_{xc}(\rho_{el}(\mathbf{r})) = -\frac{3}{4}\left(\frac{9}{4\pi^2}\right)^{1/3}\frac{1}{r_s(\mathbf{r})} - 0.0333\, G\left(r_s(\mathbf{r})/11.4\right). \tag{6}$$

Here $r_s(\mathbf{r}) = (3/4\pi\rho_{el}(\mathbf{r}))^{1/3}$ is a *local* Wigner-Seitz radius, while $\rho_{el}(\mathbf{r})$ is the electron density in the cluster, and the function $G(x)$ is defined by following relation:

$$G(x) = (1+x^3)\ln\left(1+\frac{1}{x}\right) - x^2 + \frac{x}{2} - \frac{1}{3}. \tag{7}$$

The exchange-correlation energy density $\epsilon_{xc}(\rho_{el}(\mathbf{r}))$, defines the LDA exchange-correlation potential $V_{xc}(\rho_{el}(\mathbf{r}))$ as

$$\begin{aligned} V_{xc}(\rho_{el}(\mathbf{r})) \;=\; & \frac{\delta\left[\rho_{el}(\mathbf{r})\epsilon_{xc}(\rho_{el}(\mathbf{r}))\right]}{\delta\rho_{el}(\mathbf{r})} = \\ & -\left(\frac{9}{4\pi^2}\right)^{1/3}\frac{1}{r_s(\mathbf{r})} - 0.0333\;\ln\left(1+\frac{11.4}{r_s(\mathbf{r})}\right). \end{aligned} \tag{8}$$

The Hartree-Fock (4) and LDA (5) equations have been solved in the system of the prolate spheroidal coordinates [74] as a system of coupled two-dimensional second order partial differential equations. The partial differential equations have been discretized on a two-dimensional grid and the resulting system of linear equations has been solved numerically by the successive overrelaxation method [75]. The third dimension, the azimuthal angle has been treated analytically.

An important characteristic of the cluster, which defines its stability is the total energy $E_{tot}(N,\delta)$. The total energy depends on the size N of the cluster and its core deformation δ. The total energy $E_{tot}(N,\delta)$ is equal to the sum of the electrostatic energy of the ionic core $E_{core}(N,\delta)$ and the energy of the valence electrons $E_{el}(N,\delta)$:

$$E_{tot}(N,\delta) = E_{core}(N,\delta) + E_{el}(N,\delta). \tag{9}$$

The electrostatic energy of the cluster ionic core is equal to

$$E_{core}(N,\delta) = \frac{1}{2}\int_V \rho(\mathbf{r})U(\mathbf{r})\mathrm{d}\mathbf{r}. \tag{10}$$

In the HF approximation, the electronic energy $E_{el}(N,\delta)$ is given by the general expression [68]:

$$\begin{aligned} E_{el}^{HF}(N,\delta) \;=\; & \sum_a < a \mid -\Delta/2 + U \mid a > + \\ & \frac{1}{2}\sum_{abk} q_a q_b \left[c(abk)F^k(a,b) + d(abk)G^k(a,b)\right], \end{aligned} \tag{11}$$

where a and b run over all shells. The values $F^k(a,b)$ and $G^k(a,b)$ in the Eq. (11) are the Coulomb and exchange Slater integrals, q_a and q_b are the occupation numbers for orbitals a and b, respectively. The Hatree-Fock coefficients $c(abk)$ and $d(abk)$ for the Coulomb and exchange energy contributions depend on the occupation numbers (see for details [68]).

In the framework of LDA the electronic energy of the system is given by [69, 70]:

$$E_{el}^{LDA}(N,\delta) = \sum_a < a \mid -\Delta/2 + U \mid a > + \frac{1}{2}\int \frac{\rho_{el}(\mathbf{r})\rho_{el}(\mathbf{r}')}{|\mathbf{r}-\mathbf{r}'|}\mathrm{d}\mathbf{r}\mathrm{d}\mathbf{r}' + \int \rho_{el}(\mathbf{r})\epsilon_{xc}(\rho_{el}(\mathbf{r}))\mathrm{d}\mathbf{r}, \quad (12)$$

where the latter term represents the exchange-correlation energy.

C. All-electron *ab initio* Hartree-Fock and LDA calculations

When performing all-electron *ab initio* Hartree-Fock or LDA calculations for metal clusters, one has to solve equations which are symbolically the same to the Hartree-Fock (4) and the Kohn-Sham (5) equations initially written for the jellium model case. In *ab initio* calculations, instead of using the spheroidal jellium parameterization (3) for the distribution of the ionic charge density and solving the equations only for the valence electrons, one has to deal with the exact Coulomb forces of all the ions and to solve equations (4) or (5) assuming that all electrons are present in the system. The explicit form of the exchange-correlation density functional in equations (5) can be chosen differently. There are many different functional forms, although there is no unique one. For example in [3], the *ab initio* results have been obtained with the use of the gradient-corrected Becke-type three-parameter exchange functional [76] paired with the gradient-corrected Lee, Yang and Parr correlation functional (B3LYP) [71, 77]. The post Hartree-Fock theories accounting for many-electron correlations, such as for example the Møller-Plesset perturbation theory of the fourth order (MP4) [78] have also been used in [3] for metal cluster simulations.

In this paper we do not present the explicit forms of these functionals and omit the discussion of the methods used for the solution of the Hartree-Fock and LDA equations in the *ab initio* framework. Instead, we refer to the papers, where these functionals and methods are presented (see, e.g., [3, 76, 77, 78, 79, 80, 81, 82] and references therein).

III. NUMERICAL RESULTS AND DISCUSSION

In this section we present the results of systematic numerical calculations performed for the small sodium clusters in the size range $N \leq 20$ on the basis of deformed Hartree-Fock and LDA jellium model. We determine the binding energies per atom, ionization potentials and cluster deformations. These Hartree-Fock and LDA results are compared with each other, with the available experimental data, and with the results derived from the *ab initio* theoretical framework. This comparison elucidates the important role of many-electron correlations in metal clusters and establishes the level of applicability of the deformed jellium model.

A. Total cluster energy minimization

In the Hartree-Fock and LDA jellium models the total cluster energy (11) and (12) depends on the deformation parameter δ introduced in (1).

Varying the total cluster energy on δ one can find its minimum at certain δ for each electron configuration considered. This value of δ corresponds to the stable geometrical configuration of the cluster.

In figures 1 and 2 we present the total cluster energy per atom $E_{tot}(N,\delta)/N$ calculated as a function of deformation parameter δ for the neutral and singly charged sodium clusters in the size range $N \leq 20$.

Solid lines in figures 1 and 2 present $E_{tot}(N,\delta)/N$ for those electronic configurations of clusters, that result in the absolute minimum of the total cluster energy. The δ-value corresponding to the minimum of $E_{tot}(N,\delta)/N$ characterizes the cluster shape at the equilibrium point. Dashed curves show $E_{tot}(N,\delta)/N$ for the electronic configurations providing the energy minimum the most closely located to the absolute minimum of the total energy. These figures demonstrate that for many clusters with open electron shells both oblate and prolate isomers are possible and have close energies. The type of deformation that develops in the cluster is determined by the type of the corresponding electronic configuration. If the electronic orbitals characterizing the chosen electronic configuration are alongated with respect to the cluster axis of symmetry then the prolate deformation of the ionic jellium background is preferable. In the opposite case, when electronic orbitals lay mostly at the

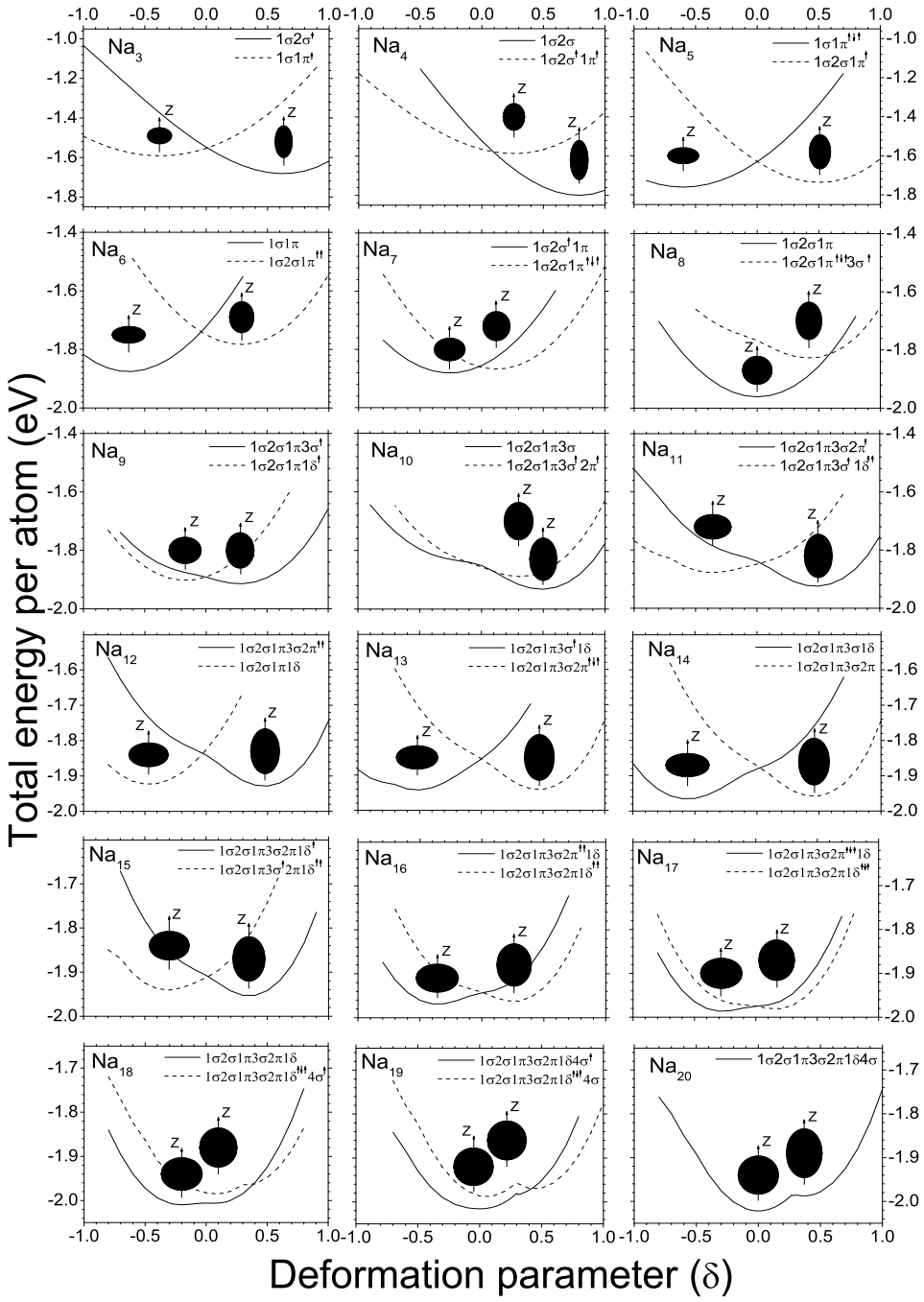

FIG. 1: Total energies per atom of neutral sodium clusters versus deformation parameter δ calculated in the LDA deformed jellium model for different electronic configurations. Solid lines show results for those electronic configurations of clusters, that result in the absolute minimum of the total cluster energy. Dashed curves show $E_{tot}(N,\delta)/N$ for the electronic configurations providing the energy minimum the most closely located to the absolute minimum of the total energy. Cluster images represent correctly the relative cluster sizes, as well as type and value of cluster

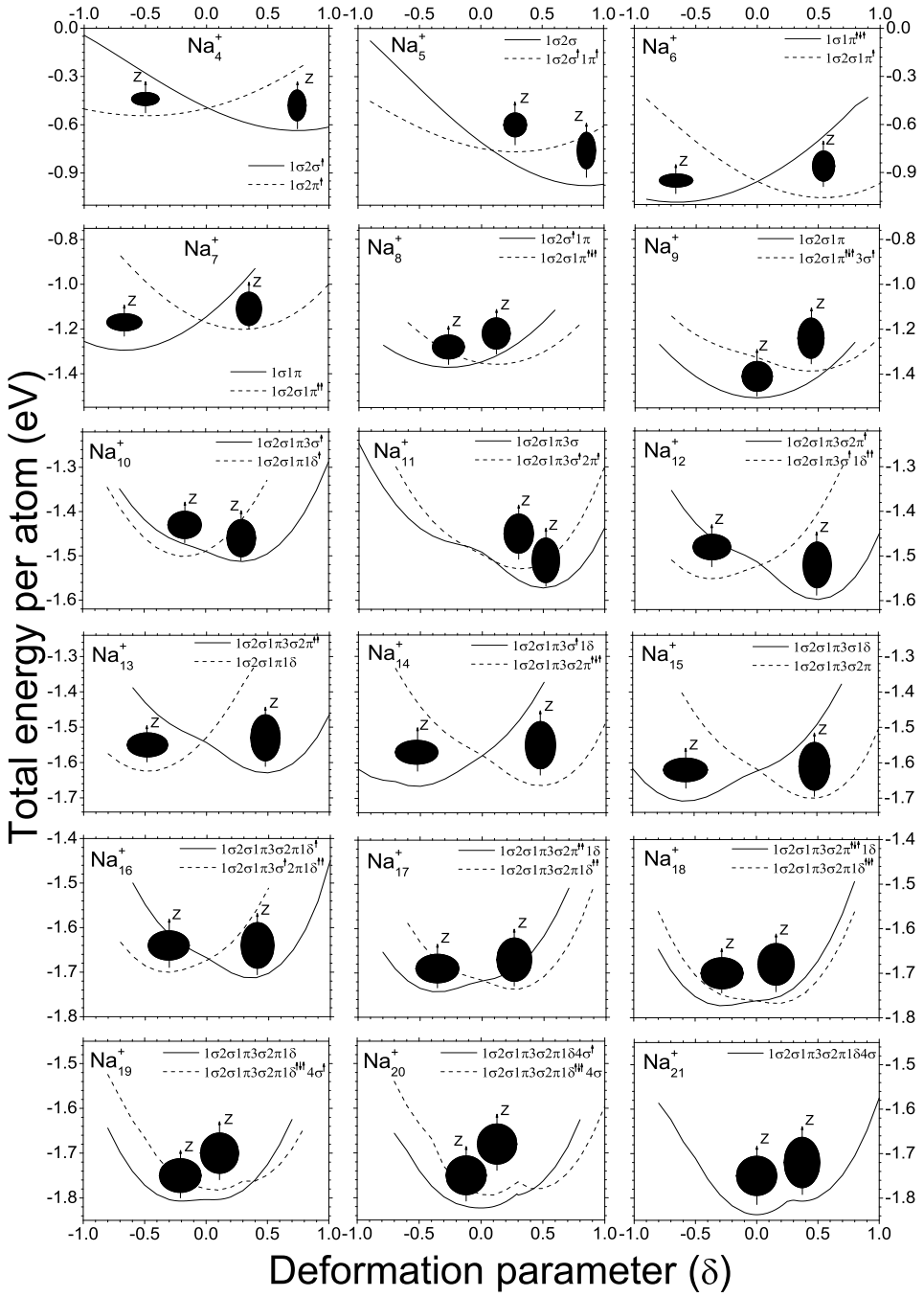

FIG. 2: The same as Fig. 1, but for the singly charged sodium cluster ions.

plane perpendicular to the cluster axis of symmetry the oblate deformation of the cluster becomes energetically more favorable.

It is interesting that the deformed jellium model predicts the existence of a non-spherical isomer for the Na_{20} magic cluster. So for Na_{20}, the second minimum in $E_{tot}(N,\delta)/N$ arises at $\delta \approx 0.37$, while the electronic configuration keeps the same. In spite of the fact that this second local minimum is energetically unfavorable, this prediction is qualitatively correct, because it corresponds to the result of *ab initio* calculations [3], which prove the existence of the two cluster isomers (pyramid and deformed structure based on the two linked icosahedrons) with the close energies. The pyramid cluster isomer possesses the tetrahedral group of symmetry, which is rather high. Thus, this isomer is analogous to the spherical cluster in the jellium picture. The deformed icosahedral structure corresponds to the prolate jellium cluster configuration. This correspondence would probably be even better if one allows the tri-axial deformations in the jellium approach.

The physical reason for the non-monotonous behaviour of the total energy $E_{tot}(N,\delta)/N$ with increasing the deformation parameter δ is the strong mixing of the highest occupied 4σ state with the unoccupied 5σ state. These levels exhibit a rather peculiar behaviour with the deformation parameter δ avoiding each other at $\delta \approx 0.37$. Such an avoided crossing-point is linked to the Wigner's no-crossing theorem [83], which states that two energy levels of the same symmetry cannot cross. Thus, the strong interaction of the 4σ state with the more prolate type 5σ state results in the appearance of the second minima at $\delta \approx 0.37$ for Na_{20} cluster.

Figure 2 demonstrates that similar behaviour of the total energy upon deformation parameter observe for singly charged cluster ions. This figure shows that in the jellium approach the closed shell cluster ions, Na_9^+ and Na_{21}^+, have the spherical shape, $\delta = 0$, at the equilibrium point, similarly to the neutral magic clusters Na_8 and Na_{20}.

B. Cluster deformations

In the axially deformed jellium model clusters can either be spherical or have a shape of ellipsoid of revolution (spheroid). The spheroidal shape can be of the two types prolate or oblate, depending on the sign of the deformation parameter δ introduced in (1). In the *ab intio* approach, the cluster shape is determined by the optimized coordinates of all the ions

and it can be characterized by the tensor R_{ij}

$$R_{ij} = \sum x_i x_j \tag{13}$$

Here, the summation is performed over all ions in the system. The principle values of this tensor R_{xx}, R_{yy} and R_{zz} define the dimensions R_x, R_y and R_z of the ionic charge distribution in the cluster along the principle axes x, y and z. Note that tensor R_{ij} is closely connected with the cluster moment of inertia tensor and the quadrupole moment tensor of the ionic distribution.

The tensor R_{ij} can also be defined for the jellium model. In this case, sum in (13) should be replaced by the integral and the integration to be performed over the homogeneous spheroidal distribution of the ionic density in the cluster. Then, the principal values of the tensor R_{ij} can easily be determined. The result of this calculation reads as

$$R_{xx} = R_{yy} = \frac{b^2}{5}N, \qquad R_{zz} = \frac{a^2}{5}N. \tag{14}$$

Here, a and b are the principle diameters of the spheroid defined in (1).

In figure 3, we present the principle values R_{xx}, R_{yy} and R_{zz} calculated for the neutral sodium clusters with $N < 20$ in the framework of the deformed jellium model according to (14). The diameters a and b have been determined by minimizing the total cluster energy in the LDA approximation (12) as explained in the previous subsection. This calculation has been performed with $r_s = 4.0$ (Fig. 3a), which corresponds to the density of the bulk sodium, and with optimized value of the Wigner-Seitz radius (Fig. 3b). The cluster energy minimization on Wiger-Seitz radius will be discussed in section III F in more detail. The LDA deformed jellium model results are shown in figure 3 by the filled triangles. The filled triangles pointing up correspond to R_{xx}=R_{yy}, while those pointing down to R_{zz}. The opened triangles are the results of the all-electron *ab initio* framework derived in [3] with the use of the B3LYP density functional. The opened triangles pointing up and down show R_{xx} and R_{zz} respectively, while the opened triangles pointing right represent R_{yy}. In figure 4 we present the results of similar calculations performed for singly charged ions. The notations used in figure 4 are the same as in figure 3.

Comparison of the results presented in figures 3 and 4, demonstrate that the optimization of the cluster energy on the Wigner-Seitz radius does not change much the neutral cluster

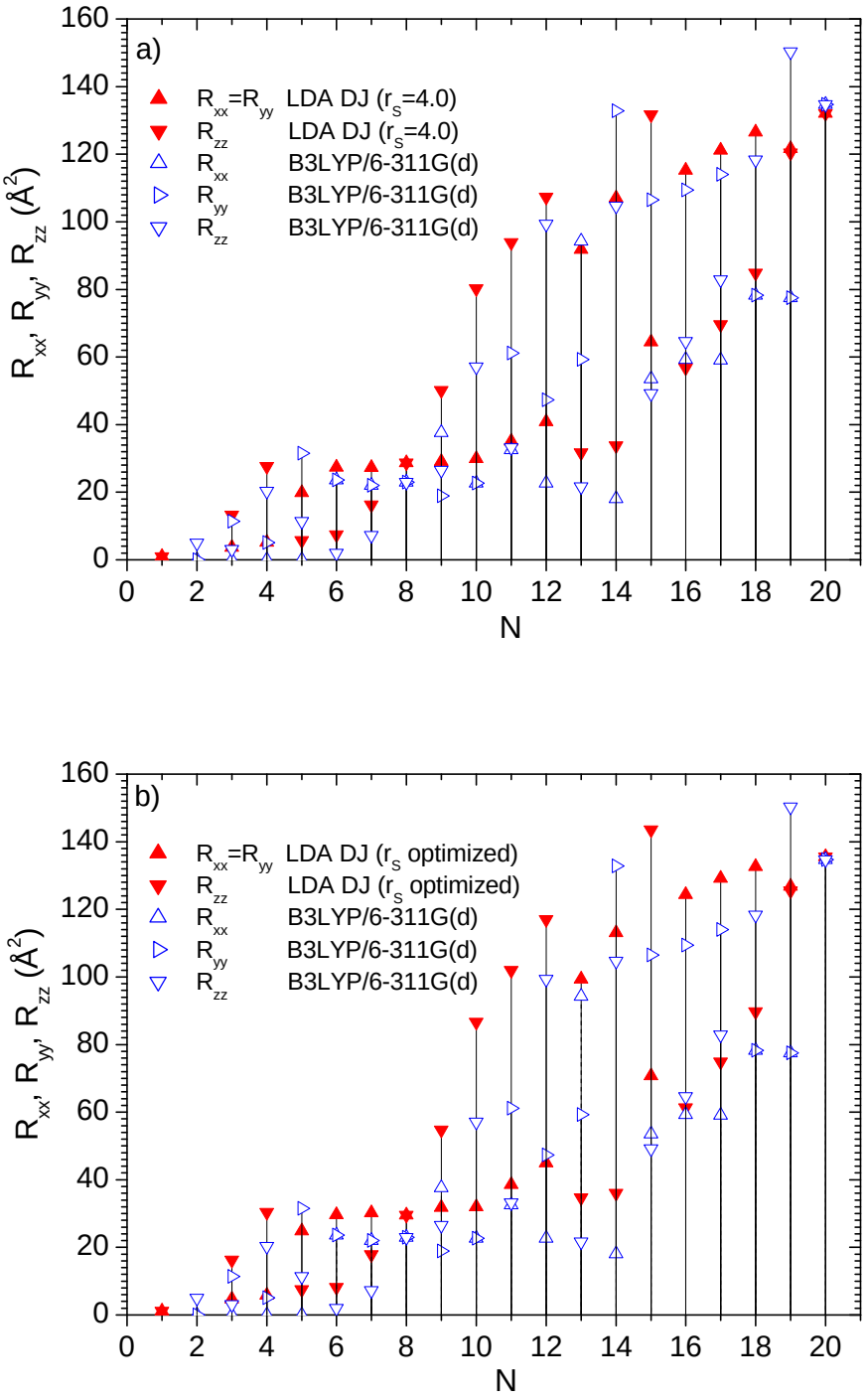

FIG. 3: The principal values of the tensor R_{ij} for neutral sodium clusters without Wigner-Seitz radius optimization (a) and with optimization on r_s (b) as a function of cluster size calculated in the LDA deformed jellium (LDA DJ) model (filled triangles) and *ab initio* B3LYP framework [3] (opened triangles).

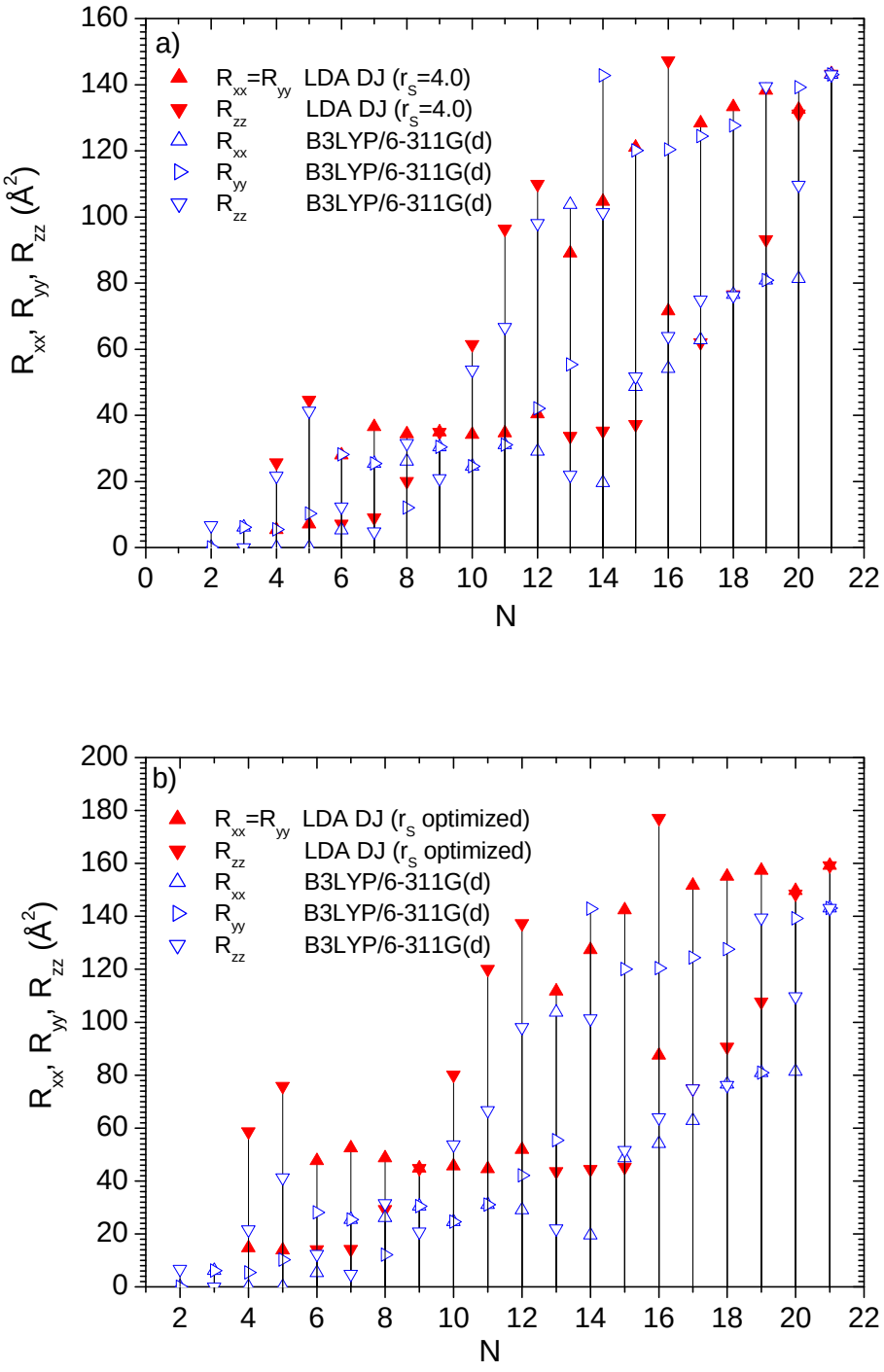

FIG. 4: The same as Fig. 3, but for singly charged sodium clusters.

geometries. For cluster ions, the alteration of the cluster shape with the variation of the Wigner-Seitz radius is more noticeable, although it does not improve the agreement of the jellium model and *ab initio* results. This comparison demonstrates that the Wigner-Seitz radius variation in the jellium model does not actually improve the quality of the model.

Figures 3 and 4 demonstrate rather good agreement of the jellium model and *ab initio* results. In most of the cases the jellium model predicts correctly the type of the dominant cluster deformation, prolate or oblate one. Of course, *ab initio* calculations include tri-axial deformations of the cluster, which turned out to be noticeable for the clusters with the open subshells and play important role for clusters like $Na_{12} - Na_{14}$, Na_{17}, Na_{13}^{+}, Na_{14}^{+}, Na_{20}^{+}. The axially symmetric deformed jellium model does not take into account tri-axial deformations and thus in this case always $R_{xx} = R_{yy}$.

The axially symmetric jellium model gives the wrong type of deformation in the open shell clusters, like Na_5, $Na_{16} - Na_{19}$, Na_6^{+}, $Na_{17}^{+} - Na_{20}^{+}$. However, it is necessary to note that for all these clusters there are almost degenerate oblate and prolate isomers within the axially symmetric jellium model, as it is shown in figures 1 and 2 and in tables I and II (see Appendix). Thus, accounting for tri-axial deformations in these clusters plays the crucial role as it becomes clear from the comparison of the jellium and *ab initio* results.

For the magic clusters Na_8 and Na_{20}, the principle values $R_{xx} = R_{yy} = R_{zz}$ are almost identical in both approaches, which demonstrates the closeness to the sphericity of the *ab initio* magic cluster shapes. Note that for the magic cluster ion, Na_9^{+}, some small deformation remains in the *ab initio* approach, while in the jellium approach it turns out to be spherical. This demonstrates that the ionic framework of the cluster is not that deformable as it follows from the jellium model.

In Appendix, we compiled in tables the optimized Wigner-Seitz radii r_s, total energies per atom $E_{tot}(N, \delta)/N$, deformation parameters δ and the second derivatives of the total energy on cluster deformation at the δ-point corresponding to minimum of the total energy. The later characteristic of the cluster, $\partial^2 E_{tot}(N, \delta)/\partial\delta^2$, is directly connected to the frequency of cluster surface vibrations (see, e.g., [44] for details). All values which are presented in the tables I and II have been calculated in the LDA deformed jellium model for neutral and singly charged clusters.

C. Binding energies per atom

In this paper we calculate the dependence of binding energy per atom in the deformed jellium model and compare it with *ab initio* results from [3]. The binding energies per atom for the neutral and singly charged clusters are defined as follows:

$$E_b/N = E_1 - E_N/N \tag{15}$$

$$E_b^+/N = \left((N-1)E_1 + E_1^+ - E_N^+\right)/N, \tag{16}$$

where E_N and E_N^+ are the total energies of a neutral and singly-charged N-atomic jellium cluster respectively.

Figure 5 shows the dependence of the binding energy per atom for neutral (Fig. 5a) and singly charged (Fig. 5b) clusters as a function of cluster size calculated in the deformed jellium model. We compare the calculated dependences with the *ab initio* results from [3] obtained by the B3LYP and MP4 methods. In figure 5 we show the jellium model results obtained with bulk and optimized values of the Wigner-Seitz radius. It is seen that the cluster optimization on the Wigner-Seitz radius brings the cluster energies down and makes them closer to the *ab initio* results.

Figure 5 demonstrates that the general trend of the curves calculated within the jellium framework turns out to be very close to the one obtained from the *ab initio* calculation. The similarity of the the jellium and *ab initio* curves is higher for $N \leq 10$. In the region $10 \leq N \leq 20$ small discrepancy in the behaviour of the curves can be attributed to the tri-axial cluster deformations taken into account in the *ab initio* approach and omitted in the axially symmetric jellium model.

Note that the jellium model results for both neutral and singly charged sodium clusters are somewhat closer to the predictions of the $MP4$ method. This method is based on the accounting of the many-electron correlations up to the fourth order of the perturbation theory and is free of any adjustable parameters.

Figure 5 demonstrates that in spite of the simplicity, the jellium model turns out to be rather reliable approximation able to reproduce reasonably well the dependence of binding energy per atom for both neutral and singly charged sodium clusters.

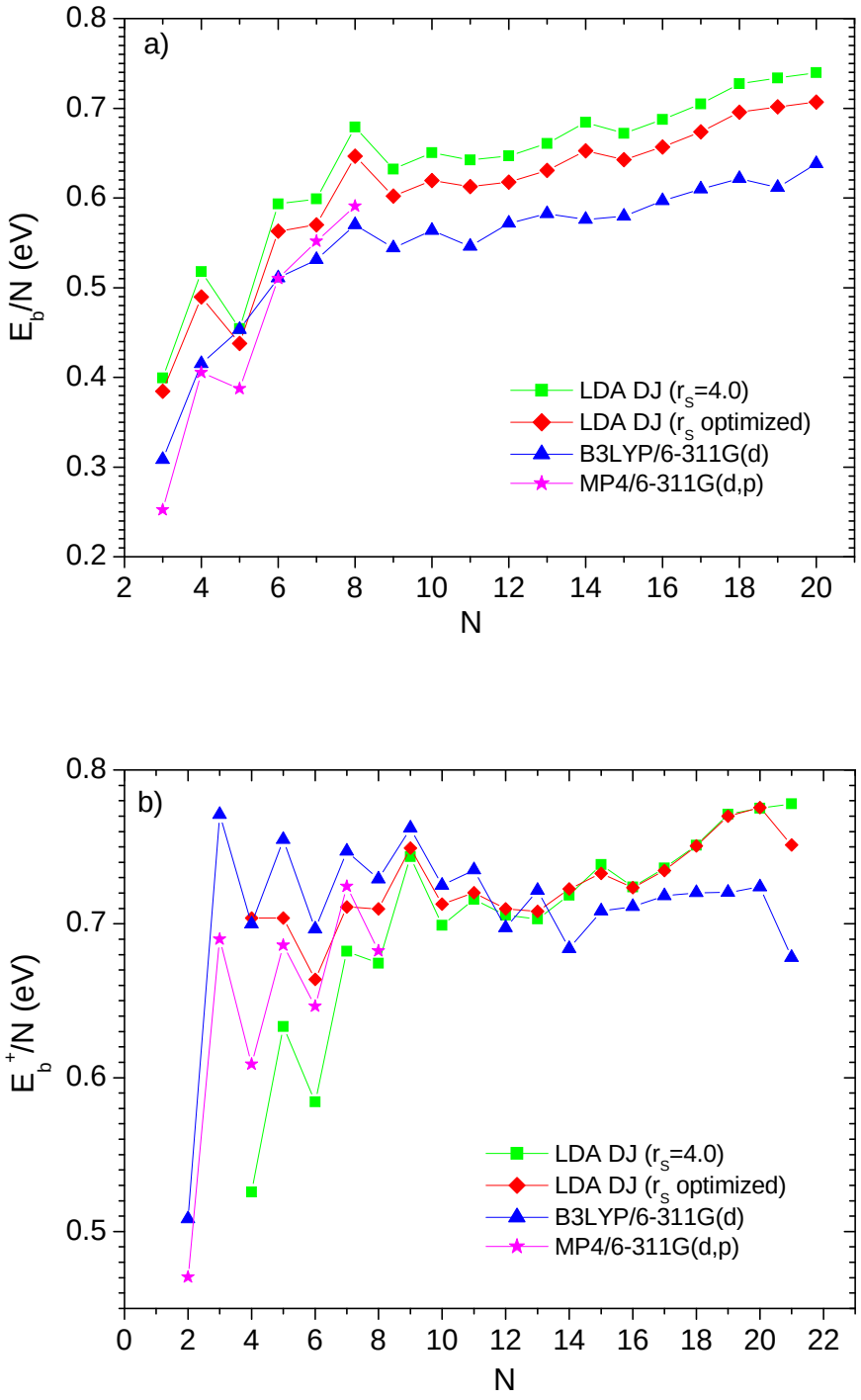

FIG. 5: Binding energy per atom for neutral (a) and singly charged (b) sodium clusters as a function of cluster size calculated in the LDA deformed jellium model and compared with *ab initio* B3LYP and MP4 results from [3].

D. On the role of exchange and many electron correlation interaction.

To illustrate the importance of the exchange and many-electron correlation interaction in the cluster, we plot on figure 6 the total energy per atom calculated both in the HF and LDA spherical jellium approximations for neutral (Fig. 6a) and singly charged (Fig. 6b) spherical sodium clusters as a function of cluster size. The spherical cluster shape was assumed in this calculation for the sake of simplicity. Figure 6 shows the significant difference between the HF and LDA results for both neutral and singly charged clusters, which is the result of the accounting for the many-electron correlation interaction within LDA.

Figure 6 demonstrates that the LDA total energy dependence possesses the local minima at the shell closings $N = 2, 8, 20$ for neutral clusters and $N = 3, 9, 21$ for singly charged ones. The HF total energy curve has the extra minima at the half-shell closings, i.e. $N = 5, 13, 19$ for neutral clusters and $N = 6, 14, 20$ for singly charged cluster ions. The appearance of these extra minima is the result of the more accurate accounting for the exchange interaction within the HF approximation. We found that with increasing cluster size within the given shell the favorable electronic configuration of the cluster changes resulting in the formation of the extra minima on the HF total energy dependence. Qualitatively, this situation can be understood on the basis of the Hund's rule which states that the lowest energy level in the system at a fixed electronic configuration is characterized by the maximum value of total spin and the maximum possible (at this spin) angular momentum. As an illustration, figure 7 shows the δ-dependencies of the total energy per atom for Na_5 cluster obtained in the Hartree-Fock (Fig. 7a) and LDA (Fig. 7b) deformed jellium model for different electronic configurations. Figure 7a clearly demonstrates that the extra minima on HF total energy curve correspond to the electronic states in which spins of all the electrons from the open shell are parallel. The LDA framework, with the exchange-correlation potential (9), which we have used in our work does not take into account the spin polarization effects and thus we found no minima on the LDA total energy curve at closing of the half filled shells (see Fig. 7b).

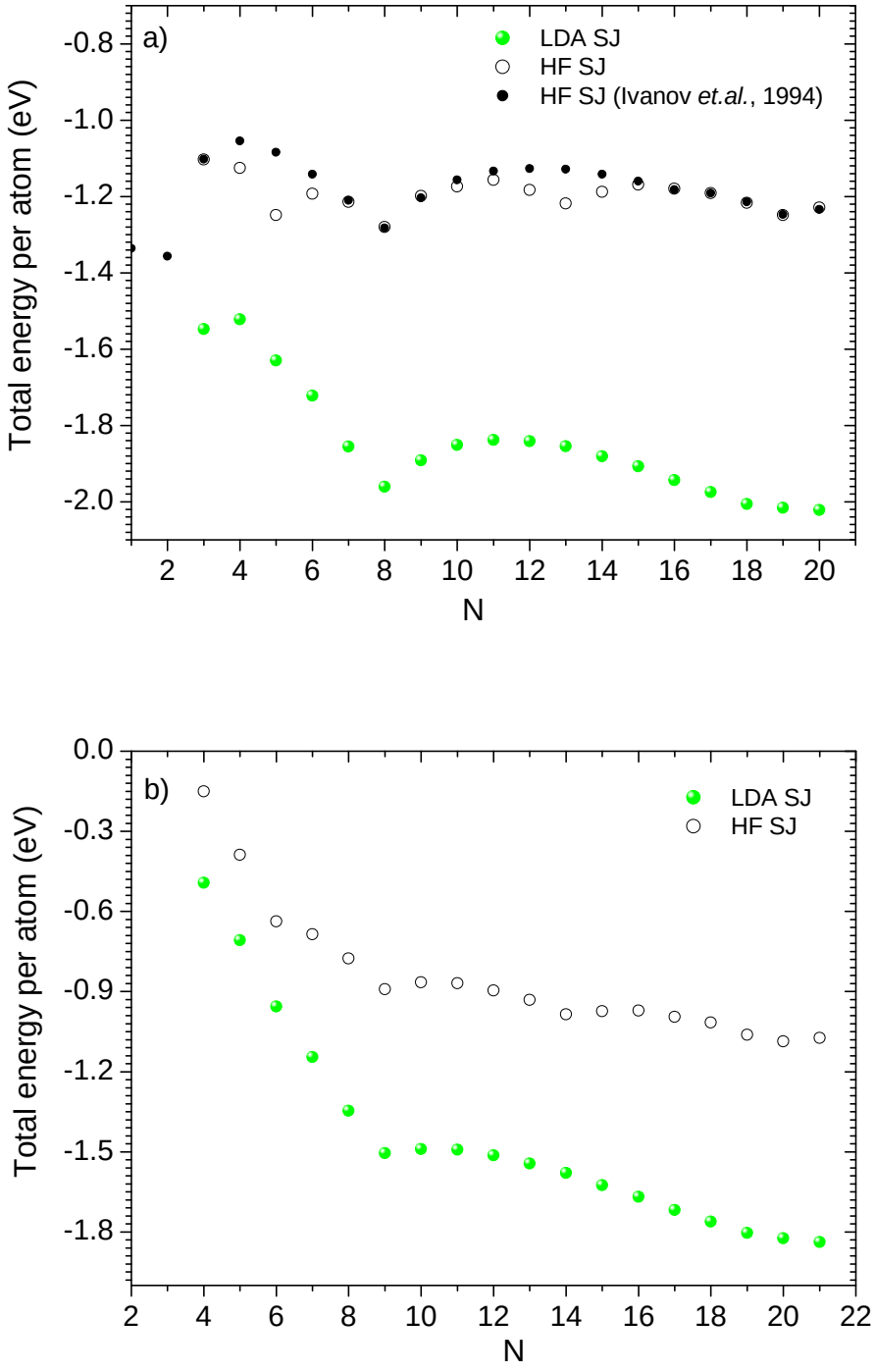

FIG. 6: Total energy per atom for spherical neutral (a) and and singly charged (b) sodium clusters calculated in the Hartree-Fock and LDA spherical jellium model (HF SJ and LDA SJ).

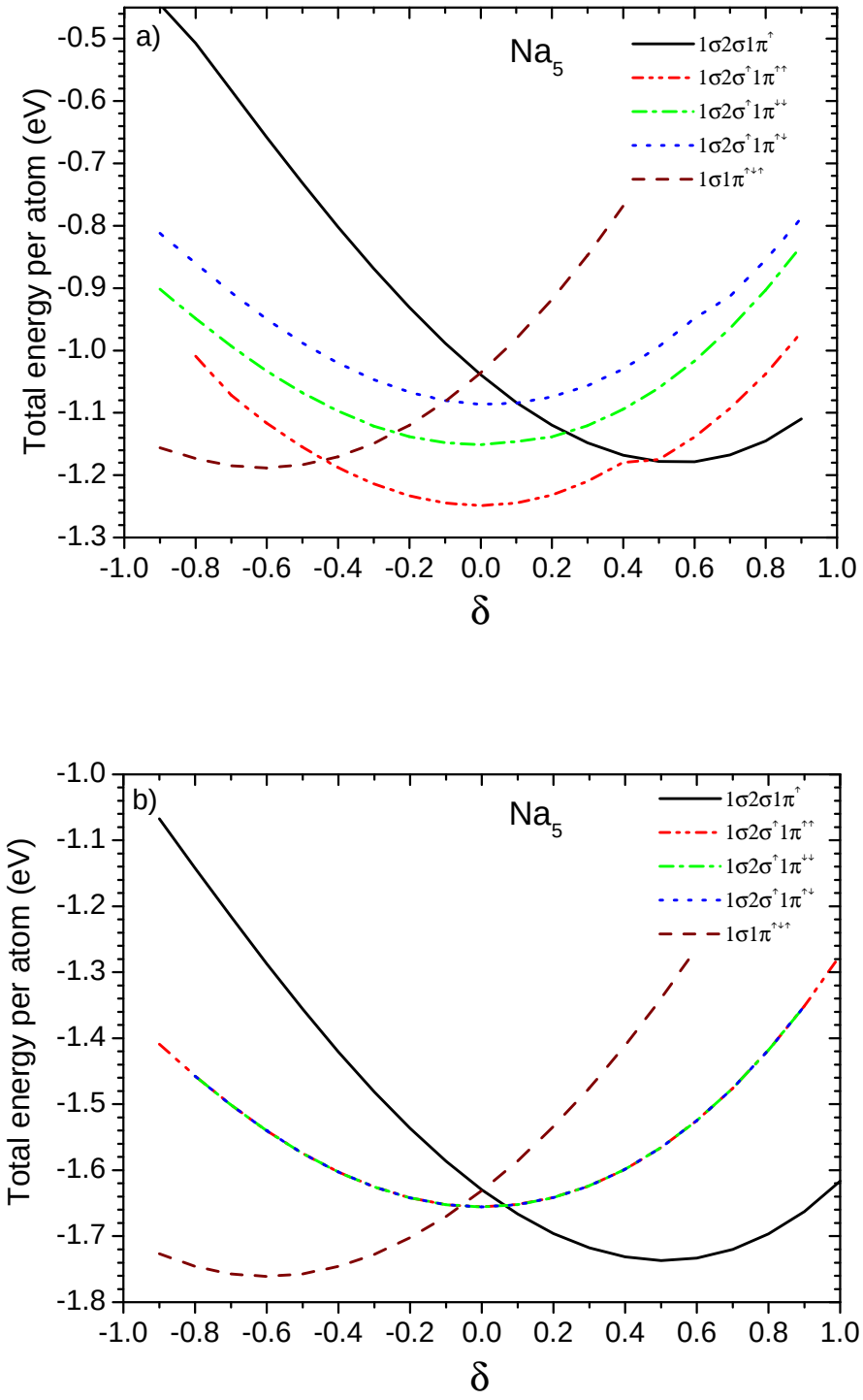

FIG. 7: Total energy per atom for Na_5 cluster versus deformation parameter δ calculated in the Hartree-Fock (a) and LDA (b) deformed jellium model for different electronic configurations.

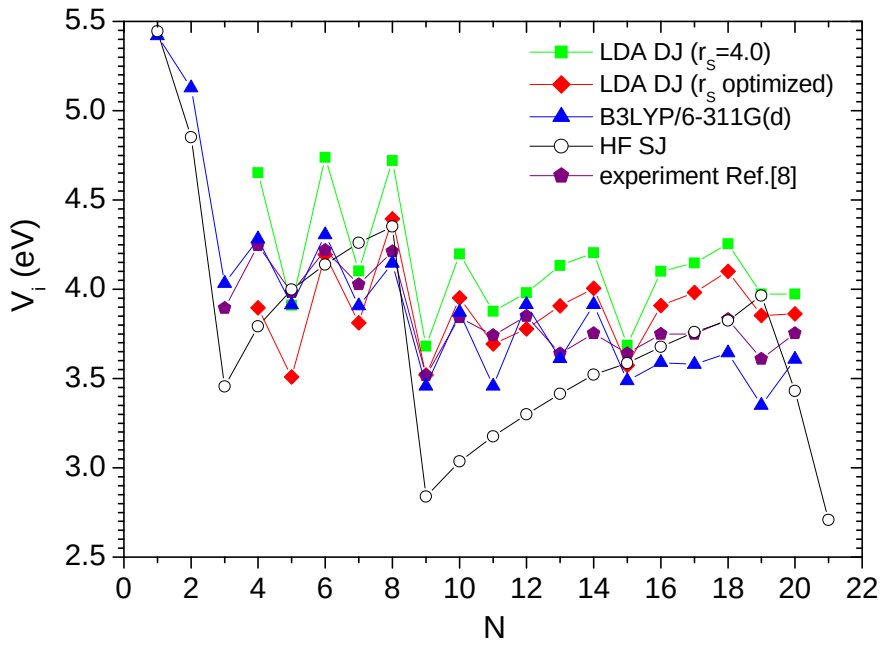

FIG. 8: Ionization potentials of neutral sodium clusters calculated in the deformed jellium model and compared with *ab initio* results from [3] and with experiment [8].

E. Ionization potentials

Another important characteristic of the cluster system is its ionization potential. The ionization potential is determined by the energy needed to take an electron out of the cluster. It is equal to:

$$V_i = E_N^+ - E_N \tag{17}$$

In figure 8, we present the ionization potential of neutral sodium clusters calculated within the jellium model as a function of cluster size. We compare the jellium model results with those obtained in [3] using *ab initio* theoretical framework and with the available experimental data [8]. This comparison demonstrates that the jellium model reproduces correctly most of the essential features of the ionization potential dependence on N. Some discrepancy, like in the region $11 \leq N \leq 14$, can be attributed to the neglection of the tri-axial deformation in the axially symmetric jellium model.

In spite of the fact that *ab initio* results are closer to the experimental points, one can state quite satisfactory agreement of the jellium model results with the experimental data, which illustrates correctness of the jellium model assumptions and its applicability to the description of sodium clusters.

Figure 8 also demonstrates the role of cluster deformations on the formation of the odd-even oscillations in the dependence of the cluster ionization potential on N. Indeed, for spherically symmetric clusters this dependence turns out to be monotonous within the range of the given shell [45] contrary to the experimental observations. Allowing for the cluster deformation and introducing a single deformation parameter δ, we have achieved much better agreement of theoretical results with the experimental data as it is clear from figure 8.

F. Wigner-Seitz radius variation

Calculations of the cluster total energy are usually performed at the certain value of the Wigner-Seitz radius r_s. The bulk value of the Wigner-Seitz radius for sodium is equal to 4.0. However, one can also perform the calculation minimizing the total cluster energy by variation of the Wigner-Seitz radius.

Figure 9 demonstrates the dependence of the optimized Wigner-Seitz radii on cluster size calculated for neutral and singly charged sodium clusters within the HF and LDA approximations. This figure shows that the alteration of the optimized r_s values is much larger for the cluster ions as compared to the neutral clusters. For neutral clusters, the optimized values are somewhat larger than the bulk value $r_s = 4.0$ in both LDA and HF approximations. The LDA dependence goes closer to the bulk limit. With increasing N this dependence approaches the bulk limit, being very close to it also for the magic numbers $N = 8$ and $N = 20$, which is another manifestation of the shell effect.

The difference between the optimized values of the Wigner-Seitz radii obtained in the HF and LDA approximations can be atributed to the manifestation of the many-electron correlation interaction in the system. To illustrate this fact, we plot in figure 10 the difference between the optimized Wigner-Seitz radii calculated in the LDA and HF approximations for neutral and singly charged sodium clusters. These dependences have the prominent peculiarities. The origin of these peculiarities is the same as for those in figure 6 (see section III D and discussion therein), although now we consider deformed cluster systems.

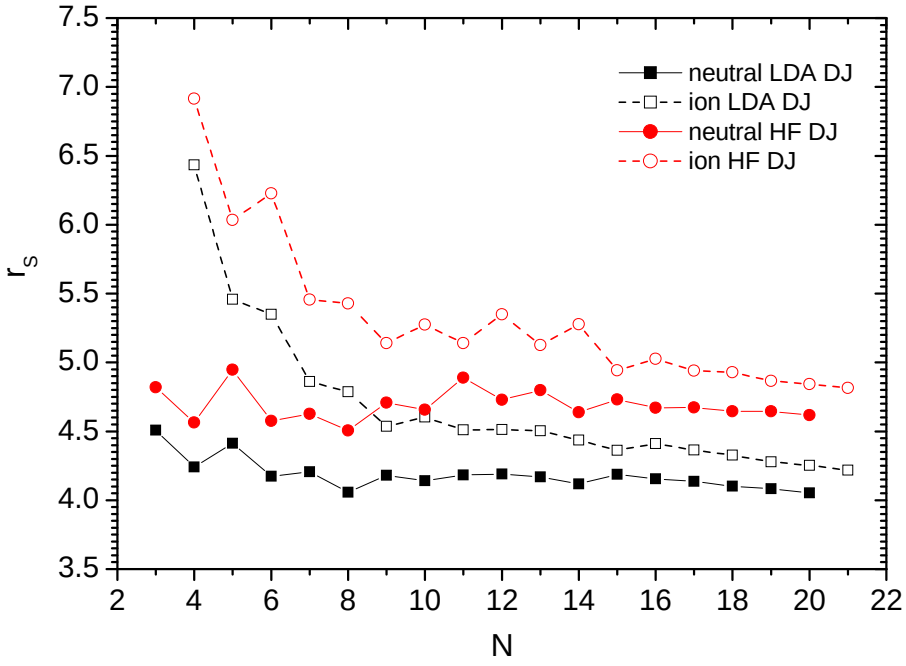

FIG. 9: Optimized Wigner-Seitz radii for neutral and singly charged sodium clusters calculated as a function of cluster size in the HF and LDA deformed jellium models.

IV. CONCLUSION

In this paper we performed systematic calculation of various characteristics of neutral and singly charged sodium clusters with $N \leq 20$ on the basis of the deformed HF and LDA jellium models. We compared the results of our calculations with the *ab initio* results obtained in [3] and with the available experimental data. From these comparisons, we have established the level of applicability of the jellium model to the description of various cluster characteristics.

Our consideration shows that the deformed jellium model provides qualitatively correct description of the sodium clusters and their ions. The quantitatively reliable results with the accuracy below than 10 per cent one can expect from the jellium model description providing one allows for the tri-axial cluster deformations.

We have performed our calculations using HF and LDA approximations. Comparison of the results of the two approaches allowed us to demonstrate the importance of the many-

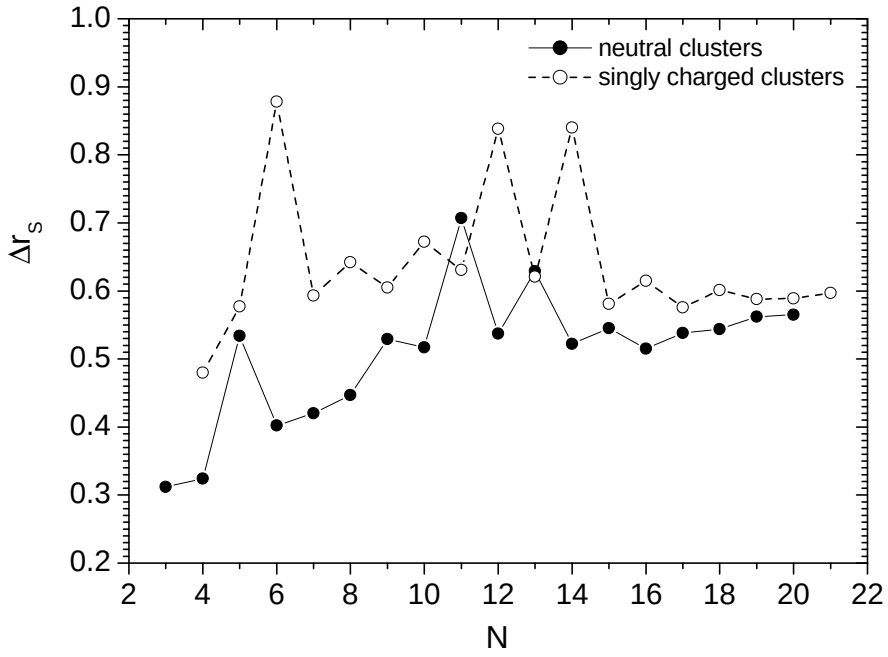

FIG. 10: Difference between the optimized values of the Wigner-Seitz radius for neutral and singly charged sodium clusters calculated as a function of cluster size in HF and LDA deformed jellium model.

electron correlations in the formation of cluster characteristics and properties.

We have performed our calculations for sodium clusters. However, most of the conclusions should be applicable to other alkali clusters, potassium for example. The level of applicability of the jellium approach to other metals, like alkali-earth, requires a separate careful consideration.

Acknowledgments

The authors acknowledge support from the Alexander von Humboldt Foundation, DAAD and the Russian Academy of Sciences (Grant 44).

*

APPENDIX A: TABLES

In Appendix, we present tables of the optimized Wigner-Seitz radii, total energies per atom, deformation parameters and the second derivatives of the total energy on cluster deformation calculated in the LDA deformed jellium model for neutral and singly charged sodium clusters.

TABLE I: Summary of the optimized Wigner-Seitz radii r_s, total energies per atom $E_{tot}(N,\delta)/N$, deformation parameters δ and second derivatives of the total energy on cluster deformation, $\partial^2 E_{tot}(N,\delta)/\partial\delta^2$, calculated at δ corresponding to the minimum of the total energy. Calculations have been performed in the LDA deformed jellium model for neutral sodium clusters.

N	r_S	Electronic configuration	E_{tot}/N (eV)	δ	$\partial^2 E_{tot}(N,\delta)/\partial\delta^2$
3	4.51	$1\sigma 2\sigma^{\uparrow}$	-1.700	0.60	0.81
		$1\sigma 1\pi^{\uparrow}$	-1.592	-0.38	0.53
4	4.24	$1\sigma 2\sigma$	-1.805	0.78	1.11
		$1\sigma 2\sigma^{\uparrow} 1\pi^{\uparrow}$	-1.588	0.26	0.69
5	4.41	$1\sigma 1\pi^{\uparrow\downarrow\uparrow}$	-1.775	-0.58	0.75
		$1\sigma 2\sigma 1\pi^{\uparrow}$	-1.753	0.49	0.90
6	4.17	$1\sigma 1\pi$	-1.878	-0.62	0.81
		$1\sigma 2\sigma 1\pi^{\uparrow\uparrow}$	-1.784	0.28	0.85
7	4.21	$1\sigma 2\sigma^{\uparrow} 1\pi$	-1.885	-0.26	0.77
		$1\sigma 2\sigma 1\pi^{\uparrow\downarrow\uparrow}$	-1.867	0.12	0.82
8	4.06	$1\sigma 2\sigma 1\pi$	-1.962	0.00	1.02
		$1\sigma 2\sigma 1\pi^{\uparrow\downarrow\uparrow} 3\sigma^{\uparrow}$	-1.828	0.42	0.83
9	4.18	$1\sigma 2\sigma 1\pi 3\sigma^{\uparrow}$	-1.917	0.27	0.78
		$1\sigma 2\sigma 1\pi 3\delta^{\uparrow}$	-1.903	-0.17	0.84
10	4.14	$1\sigma 2\sigma 1\pi 3\sigma$	-1.935	0.49	0.97
		$1\sigma 2\sigma 1\pi 3\sigma^{\uparrow} 2\pi^{\uparrow}$	-1.890	0.31	0.88
11	4.18	$1\sigma 2\sigma 1\pi 3\sigma 2\pi^{\uparrow}$	-1.928	0.48	1.03
		$1\sigma 2\sigma 1\pi 3\sigma^{\uparrow} 1\delta^{\uparrow\uparrow}$	-1.877	-0.36	0.78
12	4.19	$1\sigma 2\sigma 1\pi 3\sigma 2\pi^{\uparrow\uparrow}$	-1.933	0.47	1.07
		$1\sigma 2\sigma 1\pi 1\delta$	-1.923	-0.47	0.97
13	4.17	$1\sigma 2\sigma 1\pi 3\sigma^{\uparrow} 1\delta$	-1.946	-0.51	0.93
		$1\sigma 2\sigma 1\pi 3\sigma 2\pi^{\uparrow\downarrow\uparrow}$	-1.945	0.46	1.10
14	4.12	$1\sigma 2\sigma 1\pi 3\sigma 1\delta$	-1.968	-0.56	0.93
		$1\sigma 2\sigma 1\pi 3\sigma 2\pi$	-1.941	0.46	1.17
15	4.19	$1\sigma 2\sigma 1\pi 3\sigma 2\pi 1\delta^{\uparrow}$	-1.958	0.35	1.05
		$1\sigma 2\sigma 1\pi 3\sigma^{\uparrow} 2\pi 1\delta^{\uparrow\uparrow}$	-1.941	-0.31	0.81
16	4.16	$1\sigma 2\sigma 1\pi 3\sigma 2\pi^{\uparrow\uparrow} 1\delta$	-1.972	-0.35	0.80
		$1\sigma 2\sigma 1\pi 3\sigma 2\pi 1\delta^{\uparrow\uparrow}$	-1.964	0.26	0.98
17	4.14	$1\sigma 2\sigma 1\pi 3\sigma 2\pi^{\uparrow\downarrow\uparrow} 1\delta$	-1.989	-0.27	0.76
		$1\sigma 2\sigma 1\pi 3\sigma 2\pi 1\delta^{\uparrow\downarrow\uparrow}$	-1.963	0.16	0.82
18	4.10	$1\sigma 2\sigma 1\pi 3\sigma 2\pi 1\delta$	-2.011	-0.20	0.57
		$1\sigma 2\sigma 1\pi 3\sigma 2\pi 1\delta$	-2.008	0.06	0.93
19	4.08	$1\sigma 2\sigma 1\pi 3\sigma 2\pi 1\delta 4\sigma^{\uparrow}$	-2.016	0.00	0.51
		$1\sigma 2\sigma 1\pi 3\sigma 2\pi 1\delta^{\uparrow\downarrow\uparrow} 4\sigma$	-1.988	0.05	1.25
20	4.05	$1\sigma 2\sigma 1\pi 3\sigma 2\pi 1\delta 4\sigma$	-2.022	0.00	1.01
		$1\sigma 2\sigma 1\pi 3\sigma 2\pi 1\delta 4\sigma$	-1.990	0.37	1.02

TABLE II: The same as Tab. I, but for the singly charged sodium cluster ions.

N	r_S	Electronic configuration	E_{tot}/N (eV)	δ	$\partial^2 E_{tot}(N,\delta)/\partial\delta^2$
4	6.43	$1\sigma 2\sigma^{\uparrow}$	-0.831	0.74	0.63
		$1\sigma 2\pi^{\uparrow}$	-0.544	-0.50	0.36
5	5.46	$1\sigma 2\sigma$	-1.073	0.86	0.89
		$1\sigma 2\sigma^{\uparrow} 1\pi^{\uparrow}$	-0.771	0.28	0.56
6	5.35	$1\sigma 1\pi^{\uparrow\downarrow\uparrow}$	-1.179	-0.59	0.62
		$1\sigma 2\sigma 1\pi^{\uparrow}$	-1.159	0.54	0.77
7	4.86	$1\sigma 1\pi$	-1.341	-0.67	0.71
		$1\sigma 2\sigma 1\pi^{\uparrow\uparrow}$	-1.203	0.29	0.74
8	4.79	$1\sigma 2\sigma^{\uparrow} 1\pi$	-1.412	-0.27	0.69
		$1\sigma 2\sigma 1\pi^{\uparrow\downarrow\uparrow}$	-1.358	0.12	0.73
9	4.54	$1\sigma 2\sigma 1\pi$	-1.526	0.00	0.76
		$1\sigma 2\sigma 1\pi^{\uparrow\downarrow\uparrow}\sigma^{\uparrow}$	-1.387	-0.44	0.80
10	4.60	$1\sigma 2\sigma 1\pi 3\sigma^{\uparrow}$	-1.539	0.29	0.73
		$1\sigma 2\sigma 1\pi 3\delta^{\uparrow}$	-1.501	-0.17	0.78
11	4.51	$1\sigma 2\sigma 1\pi 3\sigma$	-1.592	0.50	0.92
		$1\sigma 2\sigma 1\pi 3\sigma^{\uparrow} 2\pi^{\uparrow}$	-1.529	0.32	0.81
12	4.51	$1\sigma 2\sigma 1\pi 3\sigma 2\pi^{\uparrow}$	-1.618	0.49	0.96
		$1\sigma 2\sigma 1\pi 3\sigma^{\uparrow} 1\delta^{\uparrow\uparrow}$	-1.551	-0.37	0.72
13	4.50	$1\sigma 2\sigma 1\pi 3\sigma 2\pi^{\uparrow\uparrow}$	-1.645	-0.48	1.01
		$1\sigma 2\sigma 1\pi 1\delta$	-1.648	0.48	0.90
14	4.44	$1\sigma 2\sigma 1\pi 3\sigma^{\uparrow} 1\delta$	-1.682	-0.53	0.87
		$1\sigma 2\sigma 1\pi 3\sigma 2\pi^{\uparrow\downarrow\uparrow}$	-1.681	0.47	1.04
15	4.36	$1\sigma 2\sigma 1\pi 3\sigma 1\delta$	-1.719	-0.57	0.87
		$1\sigma 2\sigma 1\pi 3\sigma 2\pi$	-1.701	0.46	1.09
16	4.41	$1\sigma 2\sigma 1\pi 3\sigma 2\pi 1\delta^{\uparrow}$	-1.728	0.36	1.00
		$1\sigma 2\sigma 1\pi 3\sigma^{\uparrow} 2\pi 1\delta^{\uparrow\uparrow}$	-1.700	-0.31	0.76
17	4.37	$1\sigma 2\sigma 1\pi 3\sigma 2\pi^{\uparrow\uparrow} 1\delta$	-1.755	-0.36	0.78
		$1\sigma 2\sigma 1\pi 3\sigma 2\pi 1\delta^{\uparrow\uparrow}$	-1.737	0.26	0.93
18	4.33	$1\sigma 2\sigma 1\pi 3\sigma 2\pi^{\uparrow\downarrow\uparrow} 1\delta$	-1.783	-0.27	0.66
		$1\sigma 2\sigma 1\pi 3\sigma 2\pi 1\delta^{\uparrow\downarrow\uparrow}$	-1.768	0.16	0.74
19	4.28	$1\sigma 2\sigma 1\pi 3\sigma 2\pi 1\delta$	-1.814	-0.20	0.44
		$1\sigma 2\sigma 1\pi 3\sigma 2\pi 1\delta^{\uparrow\downarrow\uparrow} 4\sigma^{\uparrow}$	-1.782	0.08	0.89
20	4.25	$1\sigma 2\sigma 1\pi 3\sigma 2\pi 1\delta 4\sigma^{\uparrow}$	-1.829	0.00	0.50
		$1\sigma 2\sigma 1\pi 3\sigma 2\pi 1\delta^{\uparrow\downarrow\uparrow} 4\sigma$	-1.795	0.05	1.20
21	4.22	$1\sigma 2\sigma 1\pi 3\sigma 2\pi 1\delta 4\sigma$	-1.816	0.00	0.97
		$1\sigma 2\sigma 1\pi 3\sigma 2\pi 1\delta 4\sigma$	-1.812	0.37	0.96

References

[1] *Metal Clusters* edited by W. Ekardt (Wiley, New York, 1999).

[2] *Atomic Clusters and Nanoparticles*, NATO Advanced Study Institute, les Houches Session LXXIII, les Houches, 2000, edited by C. Guet, P. Hobza, F. Spiegelman and F. David (EDP Sciences and Springer Verlag, Berlin, 2001).

[3] I.A. Solov'yov, A.V. Solov'yov and W. Greiner, Phys. Rev. A **65**, 053203 (2002).

[4] W.D. Knight, K. Clemenger, W.A. de Heer, W.A. Saunders, M.Y. Chou and M.L. Cohen, Phys. Rev. Lett. **52**, 2141 (1984).

[5] C. Bréchignac, Ph. Cahuzac, F. Carlier, J. Leygnier, Chem. Phys. Lett. **164**, 433 (1989).

[6] K. Selby, M. Vollmer, J. Masui, V. Kresin, W.A. de Heer and W.D. Knight, Phys. Rev. B **40**, 5417 (1989).

[7] K. Selby, V. Kresin, J. Masui, M. Vollmer, W.A. de Heer, A. Scheidemann, W.D. Knight, Phys. Rev. B **43**, 4565 (1991).

[8] W.A. de Heer, Rev. Mod. Phys. **65**, 611 (1993).

[9] M. Brack, Rev. Mod. Phys. **65**, 677 (1993).

[10] C. Bréchignac, J.P. Connerade, J.Phys.B:At.Mol.Opt.Phys. **27**, 3795 (1994).

[11] H. Haberland (ed.), *Clusters of Atoms and Molecules, Theory, Experiment and Clusters of Atoms* (Springer Series in Chemical Physics, Berlin **52**, 1994).

[12] U. Näher, S. Bjørnholm, S. Frauendorf, F. Garcias and C. Guet, Physics Reports **285**, 245 (1997).

[13] W. Ekardt, Phys. Rev. B **29**, 1558 (1984).

[14] J.L. Martins, R. Car and J. Buttet, Surf. Sci. **106**, 265 (1981).

[15] A. Hintermann and M. Manninen, Phys. Rev. B **27**, 7262 (1983).

[16] W. Ekardt, Phys. Rev. B **32**, 1961 (1985).

[17] C. Guet and W.R. Johnson Phys. Rev. B **45**, 11283 (1992).

[18] V.K. Ivanov, A.N. Ipatov, V.A. Kharchenko, M.L. Zhyzhin, Pis'ma JETPh (in Russian) **58**, 649 (1993); Phys. Rev. A **50**, 1459 (1994).

[19] K. Clemenger Phys. Rev. B **32**, 1359 (1985).

[20] W. Ekardt, Z. Penzar Phys. Rev. B **38**, 4273 (1988).

[21] W. Ekardt, Z. Penzar Phys. Rev. B **43**, 1322 (1991).

[22] B. Montag, Th. Hirschmann, J. Meyer, P.-G. Reinhard, M. Brack Phys. Rev. B **52**, 4775 (1995).

[23] M. Koskinen, P.O. Lipas, M. Manninen *Europhys. Lett.* **30**, 519 (1995).

[24] M. Koskinen, P.O. Lipas, M. Manninen Z. Phys. D: Atoms, Molecules, Clusters **35**, 285 (1995).

[25] A.G. Lyalin, S.K. Semenov, A.V. Solov'yov, N.A. Cherepkov and W. Greiner, J. Phys. B **33**, 3653 (2000).

[26] A.G. Lyalin, S.K. Semenov, A.V. Solov'yov, N.A. Cherepkov, J.-P. Connerade, and W. Greiner, J. Chin. Chem. Soc. (Taipei) **48**, 419 (2001).

[27] Th. Hirschmann, M. Brack and J. Mayer *Atomic and Nuclear Clusters*, Proceedings of the Second International Conference at Santorini, Greece, p.240, 1993.

[28] I. Hamamoto, B.R. Mottelson, H. Xie, X.Z. Zhang, Z. Phys. D **21**, 163 (1991).

[29] S.M. Reimann, M. Koskinen, H. Häkkinen, P.E. Lindelof and M. Manninen, Phys. Rev. B **56**, 12147 (1997).

[30] A. Rytkönen, H. Häkkinen and M. Manninen, Phys. Rev. Lett. **80**, 3940 (1998).

[31] H. Häkkinen, J. Kolehmainen, M. Koskinen, P.O. Lipas and M. Manninen Phys. Rev. Lett. **78**, 1034 (1997).

[32] V.M. Strutinsky, Nucl.Phys. A **95**, 420 (1967); Nucl.Phys. A **122**, 1 (1968).

[33] C. Yannouleas and U. Landman, Chem. Phys.Lett. **210**, 437 (1993).

[34] C. Yannouleas and U. Landman, Phys. Rev. B **48**, 8376 (1993).

[35] S.M. Reimann, M. Brack, and K. Hansen, Z. Phys. D **28**, 235 (1993).

[36] A. Bulgac and C. Lewenkopf, Phys. Rev. Lett. **71**, 4130 (1993).

[37] G. Lauritsch, P.G. Reinhard, J. Meyer, and M. Brack Phys. Lett. A **160**, 179 (1991).

[38] S. Frauendorf, and V.V. Pashkevich Z. Phys. D **26**, 98 (1993).

[39] C. Yannouleas, and U. Landman Phys. Rev. B **51**, 1902 (1995).

[40] S. Frauendorf, S. Reimann, and M. Brack Z. Phys. D **34**, 125 (1995).

[41] S. Frauendorf and V.V. Pashkevich Ann. Physik (Leipzig) **5**, 34 (1996).

[42] C. Yannouleas, U. Landman, and R.N. Barnett in *Metal Clusters* (Ref.[1]).

[43] L.G. Gerchikov, A.V. Solov'yov, W. Greiner, International Journal of Modern Physics E **8**, 289 (1999).

[44] L.G. Gerchikov, A.N. Ipatov, A.V. Solov'yov and W. Greiner, J. Phys. B: At. Mol. Opt. Phys. **33**, 4905 (2000).

[45] V.K. Ivanov, *Correlations in Clusters and Related Systems*, (ed.) J.-P. Connerade (Singapore: Worls Scientific, pp 73-91, 1996).

[46] G.F. Bertsch, A. Bulgac, D. Tomanek and Y. Wang, Phys. Rev. Lett. **67**, 2690 (1991).

[47] V.K. Ivanov, G.Yu. Kashenock, R.G. Polozkov, A.V. Solov'yov, J. Phys. B: At. Mol. Opt. Phys. **34**, L669 (2001).

[48] L.G. Gerchikov, J.P. Connerade, A.V. Solov'yov and W. Greiner, J. Phys. B: At. Mol. Opt. Phys. **30**, 4133 (1997).

[49] L.G. Gerchikov, P.V. Efimov, V.M. Mikoushkin and A.V. Solov'yov, Phys. Rev. Lett. **81**, 2707 (1998).

[50] L.G. Gerchikov, A.N. Ipatov and A.V. Solov'yov, J. Phys. B: At. Mol. Opt. Phys. **30**, 5939 (1997).

[51] L.G. Gerchikov, A.N. Ipatov, A.V. Solov'yov and W. Greiner, J. Phys. B: At. Mol. Opt. Phys. **31**, 3065 (1998).

[52] L.G. Gerchikov, A.N. Ipatov, R.G. Polozkov and A.V. Solov'yov, Phys. Rev. A **62**, 043201 (2000).

[53] J.P. Connerade, L.G. Gerchikov, A.N. Ipatov and A.V. Solov'yov, J. Phys. B: At. Mol. Opt. Phys. **31**, L27 (1998).

[54] J.P. Connerade, L.G. Gerchikov, A.N. Ipatov and A.V Solov'yov, J. Phys. B: At. Mol. Opt. Phys. **32**, 877 (1999).

[55] L.G. Gerchikov and A.V. Solov'yov, Z. Phys. D: Atoms, Molecules, Clusters **42**, 279 (1997).

[56] L.G. Gerchikov, A.N. Ipatov and A.V. Solov'yov, J. Phys. B: At. Mol. Opt. Phys. **31**, 2331 (1998).

[57] A. Lyalin, A. Solov'yov, W. Greiner and S. Semenov Phys. Rev. A **65**, 023201 (2002).

[58] A. Lyalin, A. Solov'yov and W. Greiner Phys. Rev. A **65**, 043202 (2002).

[59] A.V. Solov'yov, in *Atomic Clusters and Nanoparticles* (Ref.[2]).

[60] I. Boustani, W. Pewestorf, P. Fantucci, V. Bonačić-Koutecký, J. Koutecký, Phys. Rev. B **35**, 9437 (1987).

[61] V. Bonačić-Koutecký, P. Fantucci, J. Koutecký, Phys. Rev. B **37**, 4369 (1988).

[62] I. Boustani, J. Koutecký, J. Chem. Phys. **88**, 5657 (1988).

[63] V. Bonačić-Koutecký, I. Boustani, M.F. Guest, J. Koutecký, J. Chem. Phys. **89**, 4861 (1988).

[64] J.L. Martins, J. Buttet and R. Car, Phys. Rev. B **31**, 1804 (1985).

[65] F. Spiegelmann, R. Poteau, B. Montag, P.-G. Reinhard, Physics Letters A **242**, 163 (1998).

[66] F. Nogueira, J.L. Martins and C. Fiolhais, Eur. Phys. J. D **9**, 229 (1999).

[67] R. Gutiérrez, F. Grossmann, O. Knospe, R. Schmidt, Phys. Rev. A **64**, 013202 (2001).

[68] I. Lindgren and J. Morrison, *Atomic Many-Body Theory*, (Springer-Verlag, New York, Heidelberg, Berlin, 1986).

[69] P. Hohenberg and W. Kohn, Phys. Rev. B, **136**, 864 (1964).

[70] W. Kohn and L.J. Sham, Phys. Rev. A, **140**, 1133 (1965).

[71] R.G. Parr and W. Yang, *Density-Functional Theory of Atoms and Molecules*, (Oxford University Press, Oxford, New York, 1989).

[72] P. Fulde, *Electron Correlations in Molecules and Solids*, (Springer-Verlag, Berlin, 1995).

[73] O. Gunnarsson and B.I.Lundqvist, Phys. Rev. B, **13**, 4274 (1976).

[74] I.V. Komarov, L.I. Ponomarev, S.Yu. Slavianov *Speroidal and Coulomb speroidal functions*, (Nauka, Moscow, 1976).

[75] D.M. Young, *Iterative Solution of Large Linear Systems*, (Academic Press, New York, 1971).

[76] A.D. Becke, Phys. Rev. A **38**, 3098 (1988).

[77] C. Lee, W. Yang and R.G. Parr Phys. Rev. B **37**, 785 (1988).

[78] C. Møller and M.S. Plesset Phys. Rev. **46**, 618 (1934).

[79] James B. Foresman and Æleen Frisch *Exploring Chemistry with Electronic Structure Methods* (Pittsburgh, PA: Gaussian Inc, 1996).

[80] S.H. Vosko, L. Wilk and M. Nusair, Canadian J. Phys. **58**, 1200 (1980).

[81] K. Burke, J.P. Perdew and Y. Wang, in *Electronic Density Functional Theory: Recent Progress and New Directions*, Ed. J.F. Dobson, G. Vignale and M.P. Das (Plenum, 1998).

[82] L.D. Landau and E.M. Lifshitz *Quantum Mechanics* (London: Pergamon, 1965).

[83] E. Wigner and J. Meumann, Z. Phys. **51**, 844 (1929).